

Supporting Information for

Interplay between Static- and Dynamic Energy Transfer in

Biofunctional Upconversion Nanoplatfoms

Yadan Ding,<sup>†,‡,#</sup> Fei Wu,<sup>‡,§</sup> Youlin Zhang,<sup>§</sup> Xiaomin Liu,<sup>§</sup> Elinore M. L. D. de Jong,<sup>⊥</sup>  
Tom Gregorkiewicz,<sup>⊥</sup> Xia Hong,<sup>†</sup> Yichun Liu,<sup>\*,†</sup> Maurice C. G. Aalders,<sup>#</sup> Wybren Jan  
Buma,<sup>‡</sup> and Hong Zhang<sup>\*,‡,§</sup>

<sup>†</sup>*Centre for Advanced Optoelectronic Functional Materials Research, Key Laboratory for UV Light-Emitting Materials and Technology of the Ministry of Education, Northeast Normal University, Changchun 130024, P. R. China*

<sup>‡</sup>*Van 't Hoff Institute for Molecular Sciences, University of Amsterdam, Science Park 904, 1098 XH Amsterdam, The Netherlands*

<sup>§</sup>*State Key Laboratory of Luminescence and Applications, Changchun Institute of Optics, Fine Mechanics and Physics, Chinese Academy of Sciences, Changchun 130033, P. R. China*

<sup>⊥</sup>*Van der Waals-Zeeman Institute, University of Amsterdam, Science Park 904, 1098 XH Amsterdam, The Netherlands*

<sup>#</sup>*Department of Biomedical Engineering and Physics, Academic Medical Center, University of Amsterdam, 1105 AZ Amsterdam, P.O. Box 22700, The Netherlands*

\*To whom correspondence should be addressed: [h.zhang@uva.nl](mailto:h.zhang@uva.nl); [ycliu@nenu.edu.cn](mailto:ycliu@nenu.edu.cn)

## Contents

<b>Experimental Details</b>	S-3
<b>Data Analysis</b>	S-6
<b>Figure S1.</b> X-ray diffraction patterns of NaYF <sub>4</sub> : Yb <sup>3+</sup> , Er <sup>3+</sup> core and NaYF <sub>4</sub> : Yb <sup>3+</sup> , Er <sup>3+</sup> / NaYF <sub>4</sub> core-shell UCNPs	S-8
<b>Figure S2.</b> Temporal behavior of upconversion luminescence of UCNPs and UCNP-RB at 650 nm	S-9
<b>Table S1.</b> Fitted rise time for UCNPs at 540 nm, and amplitudes for UCNP-RB at 540 nm and 590 nm	S-10
<b>Table S2.</b> Bi-exponential fitting results of UCNPs and UCNP-RB at 650 nm	S-11
<b>References</b>	S-12

## Experimental details

### Materials

CF<sub>3</sub>COONa (98%), YCl<sub>3</sub>·6H<sub>2</sub>O (99.99%), YbCl<sub>3</sub>·6H<sub>2</sub>O (99.9%), ErCl<sub>3</sub>·6H<sub>2</sub>O (99.995%), oleic acid (OA, 90%), 1-Octadecene (ODE, 90%), poly(allylamine) solution (PAAM, Mw~17,000), RB (95%), 6-bromohexanoic acid (97%), *N*-(3-dimethylaminopropyl)-*N'*-ethylcarbodiimide hydrochloride (EDC, premium), and *N*-hydroxysulfosuccinimide sodium salt (NHS, >98%) were purchased from Aldrich. Y(CF<sub>3</sub>COO)<sub>3</sub>·xH<sub>2</sub>O (99.9%) was purchased from GFS chemicals. Oleylamine (80-90%) and hydrochloric acid (HCl, 37%) were purchased from Acros Organics. NaOH (>90%) was purchased from Merck KGaA, and NH<sub>4</sub>F (>98.0%) was from Alfa Aesar. All the other solvents were of analytical grade.

### Synthesis of core-shell structured NaYF<sub>4</sub>: Yb<sup>3+</sup>, Er<sup>3+</sup>/ NaYF<sub>4</sub> UCNPs

The synthesis of NaYF<sub>4</sub>: Yb<sup>3+</sup>, Er<sup>3+</sup>/ NaYF<sub>4</sub> UCNPs was based on the protocols reported by van Veggel et al.<sup>1</sup> with a few modifications. Firstly, cubic sacrificial NaYF<sub>4</sub> nanocrystals (SNCs) were prepared following the procedures of the report, but Y(CF<sub>3</sub>COO)<sub>3</sub> (2 mmol) was obtained commercially. The SNCs were dispersed in a mixture of OA (6 ml) and ODE (15 ml) as shell precursor. Secondly, core NaYF<sub>4</sub>:Yb<sup>3+</sup>, Er<sup>3+</sup> UCNPs were synthesized following the corresponding procedures but using YCl<sub>3</sub>·6H<sub>2</sub>O (0.78 mmol), YbCl<sub>3</sub>·6H<sub>2</sub>O (0.20 mmol) and ErCl<sub>3</sub>·6H<sub>2</sub>O (0.02 mmol). After reacting at 310 °C for 60 min, some of the sample (core) was collected with syringe when the reaction temperature dropped to 200 °C. Subsequently, calculated amount of SNCs was injected to the reaction mixture immediately after the temperature increased back to 310 °C, followed by ripening to yield the first core-shell sample (cs1). By repeating the processes of cooling down, collecting sample, increasing temperature, injecting SNCs, and ripening, cs2, cs3, cs4 and cs5 samples were obtained. Finally, all the six samples were

washed with ethanol for three times. The final products were dispersed in calculated amounts of cyclohexane to make the molar concentration of UCNPs the same ( $\sim 0.24$  nmol/ml, estimated by the mass concentration of UCNPs, the density of hexagonal  $\text{NaYF}_4$  and the size of these UCNPs), which was further slightly corrected based on the absorption of UCNPs at 980 nm.

### **Surface modification of UCNPs**

The UCNPs were modified with amino groups in two steps. Firstly, 1 ml of the hydrophobic oleate-capped UCNPs was mixed with 2 ml of 0.05 M HCl. After stirring for 20 h vigorously, the oleate ligand was removed from the surface of UCNPs by protonation, and the UCNPs were transferred to water layer.<sup>2</sup> With acetone and centrifugation the ligand-free UCNPs were collected. After washing twice with water/acetone, the UCNPs were dispersed in 2 ml of water, followed by addition of 60  $\mu\text{l}$  of PAAM (20 wt. % in  $\text{H}_2\text{O}$ ) and stirring for 20 h. At the end, the PAAM-UCNPs were redispersed in 2 ml of water after several times water scrubbing.

### **Coupling of UCNPs with RB photosensitizer**

To covalently bind RB molecules to UCNPs, RB hexanoic acid ester (RB-HA) was firstly synthesized according to the reported protocol.<sup>3</sup> Then, 75  $\mu\text{g}$  of RB-HA, 0.75 mg EDC and 0.75 mg NHS were reacted in a mixture of dimethyl formamide and water at room temperature for 2 h. Afterwards, 0.5 ml of PAAM-UCNPs was added, and the reaction continued for another 24 h. Finally, the UCNP-RB composites were collected by centrifugation and washed subsequently with water/ethanol and dimethyl sulfoxide (DMSO) to remove the unbound RB-HA. The final products were dispersed in DMSO. The coupling procedures were the same for all the core-shell samples, and the number of RB molecules bound to

each nanoparticle was calculated to be about  $560 \pm 50$  based on the absorption spectra of the final products.

### **Characterizations**

The morphology of the UCNPs was characterized with a FEI Verios 460 scanning electron microscope (SEM) equipped with the STEM III detector operating in the bright field mode. The crystal structure was characterized with a Philips X-ray powder diffractometer. UV-Vis absorption spectra were obtained with a Hewlett-Packard/Agilent 8453 Diode-Array Biochemical Analysis UV-Vis Spectrophotometer. The steady-state luminescence properties were characterized with a Horiba Jobin Yvon SPEX Fluorolog 3 spectrometer. Excitation of the upconversion emission was realized with a continuous wave semiconductor diode laser at 980 nm. To compare the relative emission intensities, the luminescence spectra were obtained under identical conditions for all the highly diluted UCNP and UCNP-RB samples (all the samples are diluted for the same times, and absorbance at RB absorption peak in UCNP-RB samples is  $\sim 0.1$ ). Temporal behaviors of the luminescence spectra were recorded with single-photon counting setup (Fast Comtec) configured with a Hamamatsu R9110 PMT, where excitation was with 980 nm laser pulses ( $\sim 10$  ns, 100 Hz) generated by a Nd<sup>3+</sup>:YAG laser system (Solar Inc.).<sup>4</sup>

## Data Analysis

### The shell thickness dependence of dynamic ET interaction distance

As is shown in Figure 2 in the main text, the size of the core UCNPs is about 26.6 nm, which means the  $R$  value in Figure 1A is equal to 13.3 nm. For the core-shell UCNPs with increasing shell thickness, the average size is about 28.4 nm, 32.0 nm, 35.0 nm, 39.4 nm and 44.4 nm, respectively. Correspondingly, the shell thickness is about 0.9 nm, 2.7 nm, 4.2 nm, 6.4 nm and 8.9 nm, respectively.

Because the amplitude ratio  $A_2/A_3$  of the slow- to the fast decay components in Equation (2) represents also the ratio of the numbers of emitting centers in the central area to the outer layer of UCNPs, and the emitting centers are assumed to be distributed evenly in the core of UCNPs,  $A_2/A_3$  can be expressed by the volume ratio of the central- to the outer layer area of UCNPs, which is:

$$\frac{A_2}{A_3} = \frac{\frac{4}{3}\pi r^3}{\frac{4}{3}\pi R^3 - \frac{4}{3}\pi r^3} \quad (\text{S1})$$

The calculated  $r$  for the six UCNP-RB samples (from core-RB to cs5-RB) is about 9.6 nm, 10.6 nm, 11.1 nm, 11.5 nm, 12.1 nm and 12.1 nm, respectively. It can be seen that  $r$  becomes bigger with increase of the shell thickness, however, it is noteworthy that it increases much slower than the increase of the shell thickness. When the shell thickness is *ca.* 8.9 nm, the value of  $r$  increases by only *ca.* 2.5 nm compared with the core sample. Förster distance  $R_0$  can be utilized to explain this. Following the simplified dipole-dipole interaction approximation,  $R_0 = \text{Const.} \left( \frac{k^2 \phi_D^0}{n^4} \right)^{1/6}$ , where  $\phi_D^0$  is the quantum yield of the donor in the absence of the acceptor,  $k^2$  is the dipole orientation factor,  $J$  is the overlap integral of the donor emission spectrum and the acceptor absorption spectrum, and  $n$  is the refractive index of the medium, Förster distance is dependent on the quantum yield

of UCNPs.<sup>5</sup> In the present case, the six UCNP samples have the same core, and the inert shell has no absorption at 980 nm, thus the quantum yield of these samples is roughly proportional to the luminescence intensity measured under the same conditions. The enhanced factor of upconversion luminescence from core to cs5 sample (Figure 3A) is equal to that of the quantum yield, consequently the Förster distance is lengthened, leading to a larger dynamic ET interaction distance.

### **The contribution rate of static- and dynamic ET to the total emission of RB**

In the present case,  $-A'_1\tau_{\text{rise, RB}} \ll A'_2\tau_2 + A''_3\tau_3$ , the effect of the rise process on RB emission can be neglected when considering static ET. Therefore, the contribution rate of static ET from the whole UCNP to the total emission of RB can be quantitatively given by:

$$\frac{I_{\text{static}}}{I_{\text{total}}} = \frac{A'_2\tau_2 + A''_3\tau_3}{A'_1\tau_{\text{rise, RB}} + A'_2\tau_2 + A'_3\tau_3} \quad (\text{S2})$$

Accordingly,

$$\frac{I_{\text{dynamic}}}{I_{\text{total}}} = 1 - \frac{I_{\text{static}}}{I_{\text{total}}} \quad (\text{S3})$$

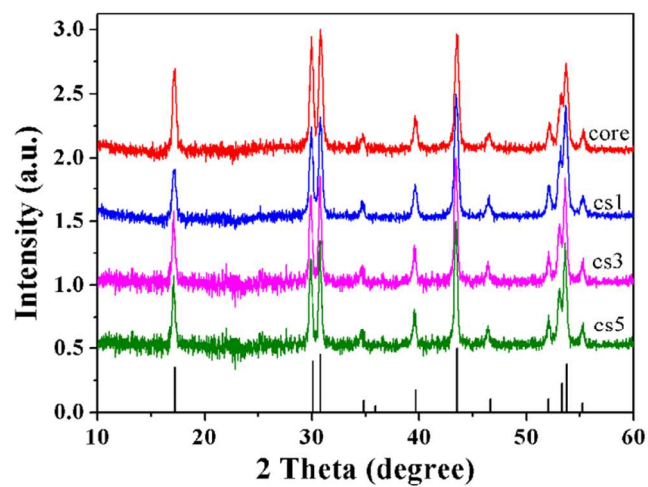


**Figure S1.** X-ray diffraction patterns of NaYF<sub>4</sub>: Yb<sup>3+</sup>, Er<sup>3+</sup> core and NaYF<sub>4</sub>: Yb<sup>3+</sup>, Er<sup>3+</sup>/NaYF<sub>4</sub> core-shell UCNPs. The standard diffraction pattern of hexagonal phase NaYF<sub>4</sub> is given for reference. (JCPDS card no. 16-0334).

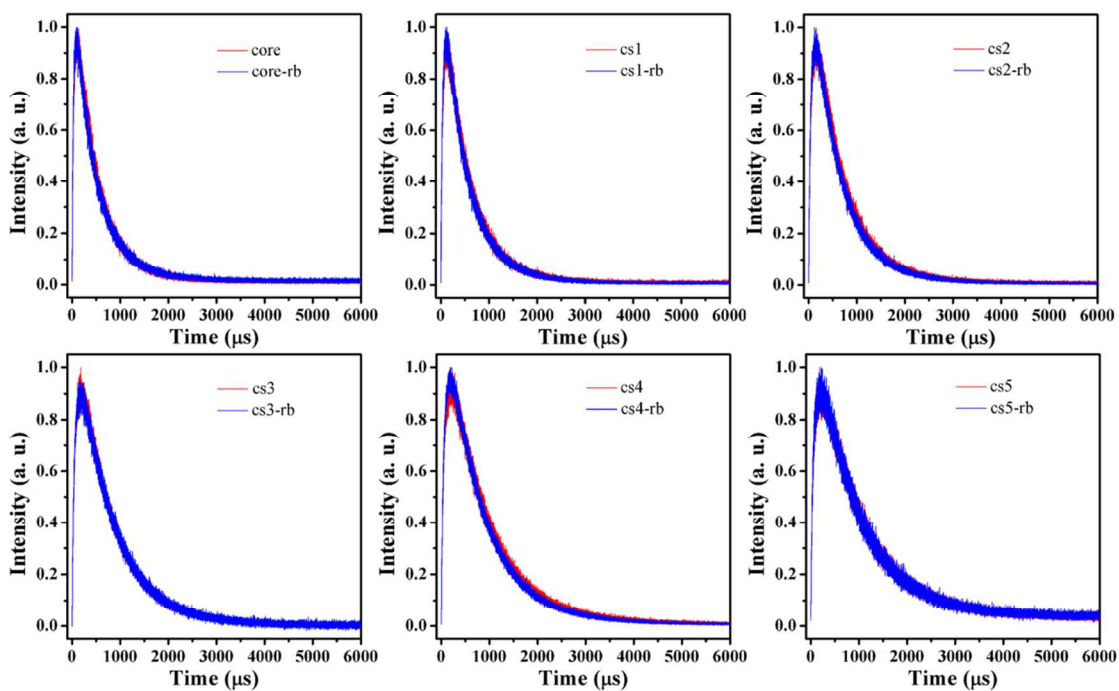


**Figure S2.** Temporal behavior of upconversion luminescence of UCNPs (red curves) and UCNPs-RB (blue curves) at 650 nm under 980 nm excitation.

**Table S1.** Fitted rise time for UCNPs ( $\tau_{\text{rise}}$ ) at 540 nm, and amplitudes for UCNP-RB at 540 nm ( $A$ ) and 590 nm ( $A'$ ) under 980 nm excitation.

	<b>core</b>	<b>cs1</b>	<b>cs2</b>	<b>cs3</b>	<b>cs4</b>	<b>cs5</b>
$\tau_{\text{rise}}/\mu\text{s}$	6.62	8.52	12.34	12.56	15.66	15.59
$A_1$	-1.07	-1.08	-1.07	-0.97	-0.98	-0.98
$A_2$	0.46	0.63	0.72	0.78	0.89	0.93
$A_3$	0.75	0.60	0.52	0.41	0.29	0.29
$A'_1$	-0.71	-0.78	-0.91	-0.57	-0.85	-0.55
$A'_2$	0.06	0.12	0.27	0.23	0.63	0.56
$A'_3$	1.02	1.02	0.87	0.50	0.49	0.36

**Table S2.** Bi-exponential fitting results of UCNPs and UCNP-RB at 650 nm.

		<b>core</b>	<b>cs1</b>	<b>cs2</b>	<b>cs3</b>	<b>cs4</b>	<b>cs5</b>
<b>UCNPs</b>	$\tau_{\text{rise}}/\mu\text{s}$	17.79	22.14	29.79	35.43	37.14	37.04
	$\tau_{\text{decay}}/\mu\text{s}$	237.80	261.56	309.82	361.34	421.62	472.54
<b>UCNP-RB</b>	$\tau_{\text{rise}}/\mu\text{s}$	14.34	19.38	26.03	32.19	34.17	36.59
	$\tau_{\text{decay}}/\mu\text{s}$	234.70	256.96	300.37	379.84	399.09	458.67

## REFERENCES

- (1) Johnson, N. J. J.; Korinek, A.; Dong, C. H.; van Veggel, F. C. J. M. Self-Focusing by Ostwald Ripening: A Strategy for Layer-by-Layer Epitaxial Growth on Upconverting Nanocrystals. *J. Am. Chem. Soc.* **2012**, *134*, 11068-11071.
- (2) Bogdan, N.; Vetrone, F.; Ozin, G. A.; Capobianco, J. A. Synthesis of Ligand-Free Colloidally Stable Water Dispersible Brightly Luminescent Lanthanide-Doped Upconverting Nanoparticles. *Nano Lett.* **2011**, *11*, 835-840.
- (3) Neckers, D. C.; Paczkowski, J. Micro-Organizational Control of Photochemical Oxidations: Rose Bengal and Derivatives (XV). *Tetrahedron* **1986**, *42*, 4671-4683.
- (4) de Boer, W.; Timmerman, D.; Dohnalova, K.; Yassievich, I. N.; Zhang, H.; Buma, W. J.; Gregorkiewicz, T. Red Spectral Shift and Enhanced Quantum Efficiency in Phonon-Free Photoluminescence from Silicon Nanocrystals. *Nat. Nanotechnol.* **2010**, *5*, 878-884.
- (5) Bednarkiewicz, A.; Nyk, M.; Samoc, M.; Strek, W. Up-conversion FRET from  $\text{Er}^{3+}/\text{Yb}^{3+}:\text{NaYF}_4$  Nanophosphor to CdSe Quantum Dots. *J. Phys. Chem. C* **2010**, *114*, 17535-17541.